Synthesis, Self-Assembled Monolayers and Alkaline Earth Metal Ion Recognition of *p-tert*-Butylcalix[4]arene Derivatives

Sheng Zhang,[a] Fayi Song,[a] and Luis Echegoyen*[a]

Keywords: Calixarenes / Metal ions / Monolayers / Molecular recognition / Self-assembly

The synthesis and self-assembled monolayer (SAM) formation of three conformational isomers of *p-tert*-butylcalix[4]crown-6 derivatives **3a**–**3c** and one *p-tert*-butylcalix[4]arene derivative (**3d**) are reported. The SAMs of these compounds were prepared and characterized by electrochemistry, reflection-absorption infrared spectroscopy (RAIRS) and contact-angle measurements. The recognition properties of these SAMs with metal cations were systematically investigated using electrochemical techniques and impedance spectroscopy. The monolayers exhibit selective binding and sensing abilities with alkaline earth metal cations such as Ca^{2+} and Ba^{2+} over alkali metal ions.

Introduction

Self-assembled monolayers (SAMs) continue to attract widespread interest because of their potential applications in materials science.[1−3] Varying the terminal functional groups on SAMs allows them to respond as sensors with many different guests. Specific analytes can be sensed by molecular recognition on the monolayer-modified surfaces. Cyclic voltammetry and impedance spectroscopy have been successfully employed to detect electrochemically active and inactive metal ions complexation on surfaces, respectively.[4,5] Many receptor molecules such as calix[4]resorcinarenes[6,7] and cyclodextrins[8] have been incorporated into SAMs. Crown-ether groups were incorporated into SAMs by Bryce et al.[9] and Reinhoudt et al.[10] and their metal-cation recognition properties were reported. We have recently prepared and investigated remarkably stable SAMs of bis-thioctic ester derivatives of oligoethylene glycols[11] and crown ether-annealed TTFs.[12] Some of these were able to detect alkali metal ion binding by means of electrochemical measurements. We also demonstrated for the first time that potassium cations could be imprinted into SAMs when the monolayer is formed in the presence of this metal cation.[13]

Calix[4]arenes, when suitably modified, can serve as host for a wide range of metal ions, and are ideal platforms or building blocks to develop receptors for molecular recognition by the incorporation of an appropriate sensory group. Remarkable examples include the potassium-selective calix[4]semitubes,[14] the tetraacetates of 1,3-alternate calix[4]arene,[15] and calix[4]crown receptors.[16] Calix[4]crown-6 compounds, in which the pentaethylene glycol unit connects with the 1,3-dialkyloxy calix[4]arene frame, exhibit highly selective complexation towards alkali and alkaline-earth metal ions. Calix[4]arene can assume four different conformations, described as 1,3-alternate, 1,2-alternate, cone and partial cone, which play crucial roles in the selectivity of the sensor for different metal cations. Calix[4]crown-6 in its 1,3-alternate conformation is particularly attractive because it exhibits remarkable efficiency to extract cesium ion from nuclear wastes.[17] For this purpose, a number of cesium-ion-selective electrodes based on 1,3-alternate-calix[4]crown-6 derivatives have been prepared and their behavior in solution reported.[18,19]

To fully realize the practical application of calix[4]crown-6 derivatives as sensors for metal cations, they need to be organized on surfaces. The incorporation of calix[4]crown-6 derivatives into SAMs to study their ion-recognition properties was reported recently.[20] Ji et al. have developed a selective cesium ion sensor based on an SAM-coated microcantilever modified by a 1,3-alternate calix[4]benzocrown-6 derivative.[20] Recently we reported the metal cation recognition properties of SAMs derived from different conformers of bis-thioctic ester derivatives of *p-tert*-butylcalix[4]crown-6.[21] In this work, we report the synthesis, SAM formation and characterization, and metal cation recognition properties of *p-tert*-butylcalix[4]arene and *p-tert*-butylcalix[4]crown-6 derivatives. Three conformational isomers of bis-thioctic ester derivatives of *p-tert*-butylcalix[4]crown-6, cone isomer **3a**, 1,3-alternate isomer **3b** and partial-cone isomer **3c** were prepared. For comparison, one bis-thioctic ester derivative of *p-tert*-butylcalix[4]arene **3d** was also synthesized. By investigating systematically the metal cation recognition properties of SAMs derived from these compounds, this work further demonstrates that olig-

[a] Department of Chemistry, Clemson University, Clemson, SC, 29634, USA
E-mail: Luis@clemson.edu
Supporting information for this article is available on the WWW under http://www.eurjoc.org or from the author.

  DOI: 10.1002/ejoc.200400130

oethylene glycol (OEG) chains attached to *p-tert*-butylcalix[4]crown-6 and *p-tert*-butylcalix[4]arene compounds have a much higher affinity for alkaline-earth metal cations than for alkali metal ions.

Results and Discussion

Synthesis

The synthetic route for **3a**−**3d** is presented in Scheme 1. The starting material, *p-tert*-butylcalix[4]crown-6 (**1**), was prepared by adapting a published procedure.[22] Kim et al. have reported that the use of only one equivalent of K_2CO_3 as base in the reaction of calix[4]arene with pentaethylene glycol ditosylate gives the desired precursor **1** in a higher yield than when using Cs_2CO_3 as base.[23] Triethylene glycol monotosylate was prepared in a high yield by reacting triethylene glycol with *p*-toluenesulfonyl chloride in the presence of silver(I) oxide and a catalytic amount of KI.[24] Reaction of the *p-tert*-butylcalix[4]crown-6 with triethylene glycol monotosylate under different conditions afforded three isomers of bis-alcohol derivatives of *p-tert*-butylcalix[4]crown-6 **2a**−**2c**. The conformations of the bis-alcohol derivatives obtained were dependent on the base and solvents used. 1,3-Alternate isomer **2b** was prepared in high yield by the reaction of triethylene glycol monotosylate with **1** in refluxing acetonitrile in the presence of Cs_2CO_3. The use of NaH as base in mixed DMF/THF (1:9) solution afforded the cone conformer **2a**. When NaH was used in anhydrous THF, the partial-cone conformer **2c** was produced as the major product in a reasonable yield. At the same time, some cone isomer **2a** was also obtained from this synthetic procedure. For the syntheses of **2a** and **2c**, it is noteworthy that very slow addition of the DMF solution of triethylene glycol monotosylate was crucial to the success of these reactions. In addition, reaction of the *p-tert*-butylcalix[4]arene with three equivalents of triethylene glycol monotosylate in the presence of K_2CO_3 gave the bis-alcohol derivative of *p-tert*-butylcalix[4]arene **2d** in 78% yield. Finally, three conformational isomers of *p-tert*-butylcalix[4]crown-6 (**3a**−**3c**) and one bis-thioctic ester derivative of *p-tert*-butylcalix[4]arene **3d** were prepared in 64%, 71%, 76% and 82% yields, respectively, by direct coupling between the corresponding bis-alcohol derivatives **2a**−**2d** and thioctic acid in CH_2Cl_2 in the presence of DCC and DMAP. This direct coupling reaction to synthesize *p-tert*-butylcalix[4]arene disulfides is straightforward and gives good yields.

All the target compounds were characterized by ^{1}H NMR, ^{13}C NMR and IR spectroscopy, mass spectrometry and elemental analysis. The ^{1}H NMR spectrum of **3b** shows

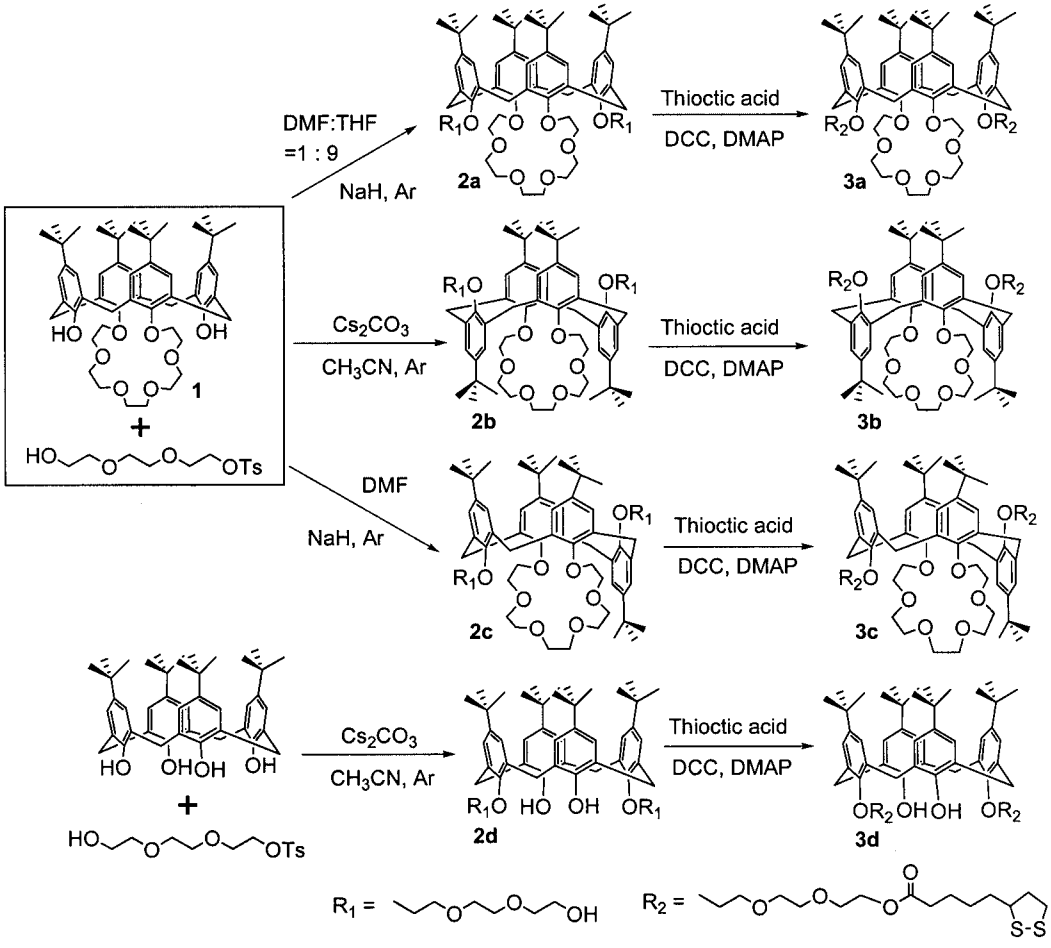

Scheme 1. Synthetic procedure for compounds **3a**−**3d**

two singlets (ratio 1:1) for the *tert*-butyl groups, a broad singlet at $\delta = 7.03$ ppm (H on the benzene ring) and a single peak with an intensity of eight hydrogens at $\delta = 3.80$ ppm corresponding to the eight methylene hydrogens connected to benzene rings, which indicate the characteristic 1,3-alternate conformation.[25,26] Also, one signal at $\delta = 38$ ppm for the four bridging methylene carbons (Ar-CH_2-Ar) in the ^{13}C NMR spectrum provides additional evidence for the 1,3-alternate conformation. The presence of typical doublets at around $\delta = 4.4$ and 3.1 ppm (overlapped with other ethylene protons) for the bridging ethylene hydrogens, two singlets (ratio 1:1) at $\delta = 1.31$ and 0.83 ppm for the *p-tert*-butyl group, two singlets at $\delta = 7.07$ and 7.27 ppm for the hydrogens on the benzene rings in the ^1H NMR spectrum, and a resonance at about $\delta = 33$ ppm in the ^{13}C NMR spectrum for compound **3a** indicate that it possesses the cone conformation. The ^1H NMR spectrum of **3c** shows three singlets (ratio 1:1: 2) for the hydrogens on the benzene rings, three pairs of doublets with an intensity ratio of 1:1:2 (two of them are mixed with other ethylene protons) for the bridging methylene protons and three singlets (ratio 1:1: 2) at $\delta = 1.32$, 1.31 and 0.83 ppm for the *tert*-butyl groups. This is in agreement with the partial-cone structure of **3c**. Two peaks at about $\delta = 34$ and $\delta = 33$ ppm in the ^{13}C NMR spectrum also suggest a partial-cone conformation of **3c**. For compound **3d**, a singlet at $\delta = 7.15$ ppm in the ^1H NMR spectrum represents the two unchanged hydroxyl groups; the presence of the doublets at $\delta = 4.3$ and 3.3 ppm in the ^1H NMR spectrum and a singlet at about $\delta = 33$ ppm in the ^{13}C NMR spectrum reveal a cone conformation for **3d**. In addition, for 1,3-alternate and cone conformers **3a**, **3b**, **3d**, only one singlet for the carbonyl group is observed at $\delta = 173.35$, 173.29 and 173.85 ppm, respectively, in the ^{13}C NMR spectra. However, two peaks for the carbonyl groups appear at $\delta = 178.49$ and 173.53 ppm in the case of the partial-cone isomer **3c**. The mass and IR spectra also confirm the structures of **3a**−**3d** very clearly. For all the target compounds, molecular ion plus Na^+ and/or K^+ peaks were observed as the parent signals in the mass spectra. Strong bands in the IR spectra are observed at around 1735 cm^{-1} for **3a**−**3d**, which are assigned to the carbonyl groups.

We further characterized the structures of the monolayers by reflection-absorption infrared spectroscopy (RAIRS). Figure 1 shows the transmission IR spectrum of **3b** and the RAIRS spectrum of the corresponding monolayer. Both of the spectra show peaks at around 2950 and 2866 cm^{-1}, assigned to the asymmetric and symmetric CH_2 stretching, respectively. For the monolayer of **3b**, a strong peak is observed for the carbonyl stretching at 1735.5 cm^{-1}, which is slightly shifted to higher wavenumbers compared to the corresponding carbonyl stretching mode in the transmission IR spectrum. Furthermore, a strong absorption band is observed at 1122 cm^{-1} attributed to the C−O−C stretching mode of the anchoring oligoethylene glycol (OEG) group. The intensity of this absorption band is obviously increased and shifted to higher frequencies in comparison with the C−O−C stretching observed in the transmission IR spectrum of **3b**. In addition, in the transmission IR spectrum of **3b**, the C=C stretching modes of the aromatic benzene rings appear at around 1560, 1474 and 1458 cm^{-1}. However, only one obvious peak at 1480 cm^{-1} is observed for the C=C stretching of the aromatic rings from the RAIRS spectrum of **3b**. These observations, especially the variations of the stretching modes of the carbonyl groups and C−O−C groups from the anchoring chains indicate that the orientation of the molecule is fixed once the monolayer is formed on the surface.

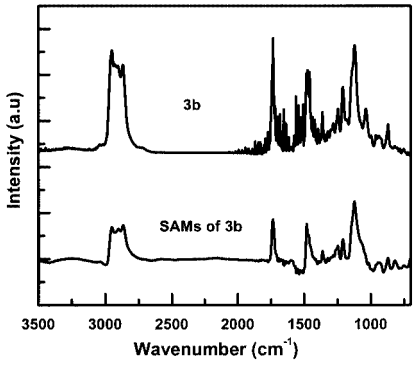

Figure 1. Transmission IR spectrum of **3b** and RAIRS spectrum of monolayer of **3b**

Characterization of the SAMs

The contact angles of these *p-tert*-butylcalix[4]arene-terminated SAMs were measured. After the monolayer of **3a** was formed on the surface, the contact angle was found to be 97 ± 2° in comparison with 44 ± 2° on bare gold. For SAMs of **3b**, **3c**, and **3d**, the contact angles with water were observed to be 83 ± 2°, 85 ± 2°, and 87 ± 2° respectively. These data indicate that hydrophobic films are formed on these gold surfaces due to the bulky *p-tert*-butyl groups and benzene rings on the calix[4]arene frame. Gupta et al. have reported contact angles of 70−74° for monolayers formed from tetrasulfide-calix[4]arene molecules with eight hydroxyl groups.[27]

Blocking Properties of the SAMs towards Electron Transfer

The extent of a blocking effect of electrochemically inactive SAMs is dependent on the existence of defects. For a monolayer with fixed thickness, the degree of electrode blocking decreases as the density of defects increases. The cyclic voltammetric response of a solution-reversible redox couple is an effective method to obtain information about the quality of the blocking monolayer. In our case, the hydrophilic probe $Ru(NH_3)_6^{3+/2+}$ was used to investigate the electrochemical blocking properties of the SAMs. A reversible redox behavior with $E^\circ_{1/2} = -0.16$ V versus Ag/AgCl was observed on bare gold electrodes. The typical CV response for the $Ru(NH_3)_6^{3+/2+}$ redox couple at a gold elec-

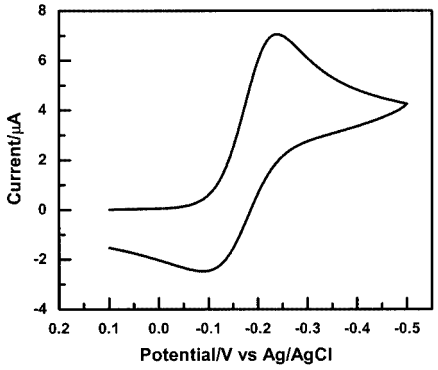

Figure 2. Cyclic voltammogram of $Ru(NH_3)_6^{3+/2+}$ in 0.1 M Et_4NCl at a gold electrode modified with SAMs of **3d** at a scan rate of 100 mV/s

trode modified with **3d** is shown in Figure 2. Some variations were observed for the different SAM-modified gold electrodes but all showed some blocking effects. Obviously, the blocking effect of the monolayer is not perfect, since a large cathodic current was observed, indicating a remaining relatively fast electron transfer at the interface. This is ascribed to either poor surface coverage or good electron permeability through the monolayer.

The cyclic voltammetric response of the redox couple can be used to study the recognition properties of the electrode modified with a suitable acceptor. It is interesting to observe from Figure 3 that addition of Ba^{2+} to the electrolyte leads to drastically reduced cathodic current at a SAM **3c** modified electrode, from 8.9 μA in the absence of Ba^{2+} to 4.3 μA in the presence of 60 mM Ba^{2+}. At the same time, the corresponding anodic current almost completely disappeared. These observations are due to the inhibition of electron transfer at the interface caused by strong repulsion between the calixcrown-bound cations (Ba^{2+}) and the positively charged $Ru(NH_3)_6^{3+/2+}$ redox couple. Similarly, addition of Ca^{2+} to the electrolyte also results in drastically decreased faradic currents for the same gold electrode. In contrast, the CV response at a **3c**-modified gold electrode shows almost no change when K^+, Na^+ or Cs^+ is added to the electrolyte solution. This means that partial-cone *p-tert*-butylcalix[4]crown-6 isomer **3c** can bind Ba^{2+} and Ca^{2+},

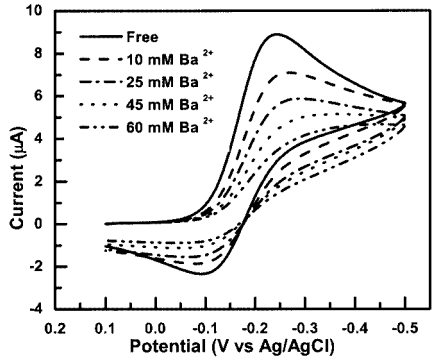

Figure 3. Cyclic voltammogram of $Ru(NH_3)_6^{3+/2+}$ in 0.1 M Et_4NCl at a gold electrode modified with SAMs of **3c** upon addition of Ba^{2+} at a scan rate of 100 mV/s

but does not effectively bind the alkali metal cations. CV blocking experiments confirm that the gold electrodes modified by SAMs of **3a** and **3d** exhibit the same recognition trend as those of **3c**; both of them bind Ba^{2+} and Ca^{2+} but not K^+, Na^+ or Cs^+. However, SAMs of **3b** can also bind Cs^+ because of its appropriate 1,3-alternate conformation but not K^+ and Na^+. Table 1 shows the variation of cathodic current for the $Ru(NH_3)_6^{3+/2+}$ redox couple at the gold electrodes modified with SAMs of **3a**−**3d** upon the addition of different metal ions.

Table 1. Change of cathodic current for the $Ru(NH_3)_6^{3+/2+}$ redox couple at SAMs of **3a**−**3d** upon the addition of 60 mM of different metal ions

	Change of cathodic current (μA)			
	SAMs of **3a**	SAMs of **3b**	SAMs of **3c**	SAMs of **3d**
Na^+	0.01	0.02	0.02	0.02
K^+	0.03	0.01	0.02	0.02
Cs^+	0.03	4.40	0.04	0.03
Ca^+	3.99	5.18	4.54	3.23
Ba^+	4.31	5.28	4.60	3.41

Ion-Binding Properties of the Monolayers Studied by Impedance Spectroscopy

To characterize electrochemically inactive SAMs without destruction of the monolayer, impedance spectroscopy is a very useful electrochemical technique.[5] If performed at the formal potential of the redox probe in solution, where the concentrations of the oxidized and reduced forms of the redox couple are equal, it allows the use of a simple Randles equivalent circuit,[28] shown in Scheme 2, to describe the impedance response. The circuit is composed of a charge-transfer resistance, R_{ct}, in series with a Warburg impedance (Q_m) and parallel to a total interfacial capacitance (Q_{dl}). These are assumed to be in series with the solution resistance R_s. From the circuit, two frequency regions can be distinguished to understand the effect of the SAMs on the CV response at the interface. In the low-frequency region, the Warburg impedance has to be taken into account, whereas at higher frequencies, the electrode reaction is totally kinetic-controlled. Under these conditions, the heterogeneous charge-transfer resistance is expected to be larger than the value of a bare gold electrode due to the blocking effect of the monolayer.

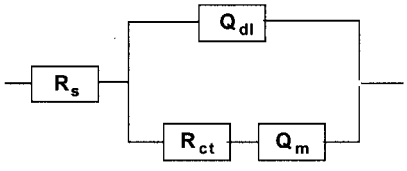

Scheme 2. Equivalent circuit used to fit the impedance data: R_s represents the solution resistance; the monolayer is described by a constant phase element, Q_{dl}, in parallet with charge-transfer resistance, R_{ct}, and another constant-phase element, Q_m, in series

The Nyqvist plot obtained on the bare gold electrode displays mainly the Warburg impedance, indicating that the redox reaction is very fast on a bare gold surface. The impedance spectra at gold electrodes modified with **3a**−**3d** in the presence of 1 mM $Ru(NH_3)_6^{3+}$ with 0.1 M tetraethylammonium chloride as the supporting electrolyte exhibit sigmoidal voltammograms with both a semicircular and a linear part in the Nyqvist plot. The charge-transfer resistance (R_{ct}) was used to investigate the ion-binding processes at the monolayer/solution interface; its value is highly dependent on the metal cations added to the electrolyte solution. Figure 4 shows the impedance response of a monolayer of **3a** upon the addition of increased [Ba^{2+}]. Addition of Ba^{2+} to the solution increases the R_{ct} value from 16.7 kΩ in the absence of Ba^{2+} to 81.8 kΩ in the presence of 80 mM Ba^{2+}. This indicates complexation of Ba^{2+} at the interface and the repulsion of the positively charged redox probe, in perfect agreement with the CV observations. The system was found to be completely reversible in that replacing the Ba^{2+}-containing solution with a metal cation free electrolyte leads to the initially determined value of R_{ct}. This same gold electrode responds similarly to Ca^{2+}. The R_{ct} value increased to 60.8 kΩ upon the addition of 80 mM of Ca^{2+}, indicating that SAMs of the cone isomer **3a** have a higher affinity for Ba^{2+} than for Ca^{2+}. However, the complex plane impedance response of SAMs of **3a** upon the addition of increased [Na^+] and [K^+] shows essentially no effect on the charge-transfer resistance; in the case of Cs^+, the R_{ct} value changes slightly.[21] These observations corroborate that sodium, potassium and cesium ions cannot bind significantly to the SAMs in these cases.

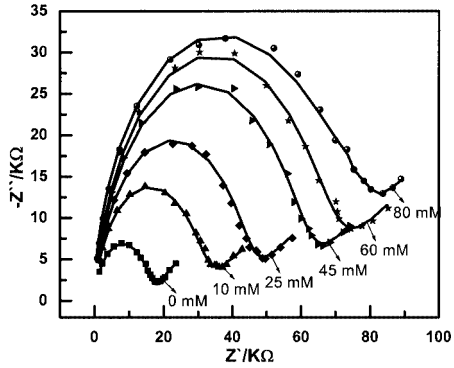

Figure 4. Impedance response of the electrode modified by SAMs of **3a** in the absence and presence of increasing [Ba^{2+}]; the solid lines represent the fits of the experimental points

The recognition ability of SAMs of **3b** for different metal cations was also systematically investigated. Like its cone isomer, SAMs of **3b** cannot bind Na^+ and K^+, but they can strongly bind Ba^{2+} and Ca^{2+}. Figure 5 shows the increase of the charge-transfer resistance at a gold electrode modified with **3b** upon the addition of increasing [Ca^{2+}]. Addition of Ba^{2+} and Ca^{2+} to the electrolyte gives rise to an increase in the value of R_{ct}, from 13.3 kΩ in the absence of metal cations to 60.1 kΩ (not shown) and 44.2 kΩ, respectively, in the presence of 80 mM Ba^{2+} and Ca^{2+}. More interestingly, an increase of the R_{ct} value was also observed when Cs^+ was added to the electrolyte at the same gold electrode.[21] The latter observation is in sharp contrast to that of **3a**. Figure 6 shows the impedance response of the monolayer of **3b** in the presence of 45 mM K^+, Cs^+, Ca^{2+} and Ba^{2+}. The R_{ct} value remained constant when K^+ was added to the electrolyte, but increased to different extents when Cs^+, Ca^{2+} and Ba^{2+} were added to the electrolyte solution. It is evident that barium cation interacts more strongly than Cs^+ and Ca^{2+}.

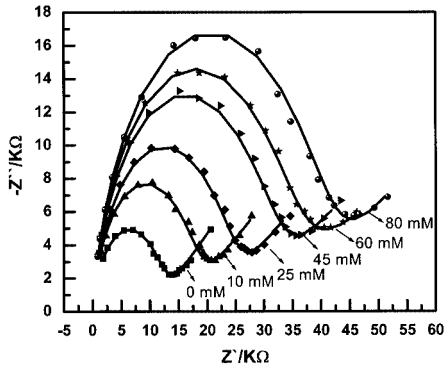

Figure 5. Impedance response of the electrode modified by SAMs of **3b** in the absence and presence of increasing [Ca^{2+}]; the solid lines represent the fits of the experimental points

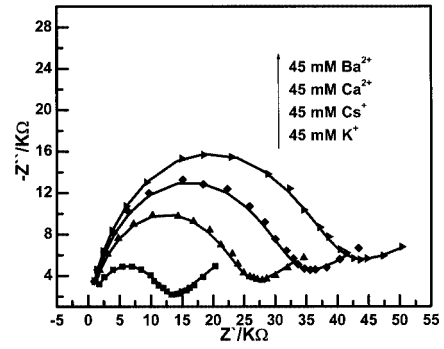

Figure 6. Comparative complex impedance plot for the SAMs of **3b** in the presence of K^+, Cs^+, Ca^{2+} and Ba^{2+} (45 mM)

Upon comparing the recognition properties of SAMs of **3a** with those of **3b**, it is fair to say that the complexation abilities of the acceptor are controlled by their conformations. In comparison with the cone isomer **3a**, the 1,3-alternate isomer **3b** has a much more favorable conformation to recognize Cs^+. In SAMs of **3b**, Cs^+ can access the crown ether moiety freely, but it has to pass through the calixarene cavity to reach the binding site in SAMs of **3a**, since the crown ether ring is buried under the *tert*-butyl groups. The conformation of **3b** couples the complexation ability of the crown ether ring with the interaction between the aromatic centers and Cs^+. This research further demonstrates the potential use of 1,3-alternate-calix[4]crown-6 derivatives as sensors and possibly to remove Cs^+ from nu-

clear wastes. On the other hand, the selectivity of SAMs of **3a** is not optimal, since it also binds Ca^{2+} and Ba^{2+}. There are two molecular domains where Ca^{2+} and Ba^{2+} can bind with *p-tert*-butylcalix[4]crown-6 derivatives **3a** and **3b** — the crown ether ring or the OEG chains.

In order to determine the relative contributions of these Ca^{2+} and Ba^{2+} binding motifs and to improve the selectivity of the sensors, we further prepared SAMs of **3c** and **3d** and investigated their metal cation recognition properties by impedance spectroscopy. Compound **3d** has a cone conformation with the OEG chains attached to the lower rim but without the crown ether ring. Like cone isomer **3a**, gold electrodes modified with SAMs of **3d** show no binding with K^+, Na^+ or Cs^+. However, addition of Ca^{2+} and Ba^{2+} increased R_{ct}, suggesting that both Ca^{2+} and Ba^{2+} can form stable complexes with SAMs of **3d**. For partial-cone isomer **3c**, one thioctic ester attached phenol group is inverted. Even though the OEG spacer is flexible, the frame of the partial-cone isomer is quite rigid. Probably only one thioctic ester can attach to the gold surfaces. Further research is underway to unravel how the SAMs actually form. Both the CV and impedance responses indicate faster electron transfer at the gold electrode modified by SAMs of **3c**, compared to those of **3a**, **3b** and **3d**. Like SAMs of **3a** and **3d**, SAMs of **3c** exhibited almost no sensing capacity for K^+, Na^+ and Cs^+; but the R_{ct} value increased from 8.05 kΩ in the absence of metal cations to 39.3 kΩ and 40.2 kΩ, respectively, when 80 mM of Ca^{2+} and Ba^{2+} were added to the electrolyte solution. Impedance responses for SAMs of **3c** in the presence of 60 mM of $[Na^+]$, $[Cs^+]$, $[Ca^{2+}]$ and $[Ba^{2+}]$ are shown in Figure 7. Apparently, Ca^{2+} and Ba^{2+} can interact with the monolayer of **3c**, but Na^+, K^+ (not shown) and Cs^+ cannot. Unlike SAMs of **3a**, **3b** and **3d**, which exhibit a higher affinity for Ba^{2+} than for Ca^{2+}, the sensing ability of SAMs of **3c** for Ca^{2+} and Ba^{2+} is similar.

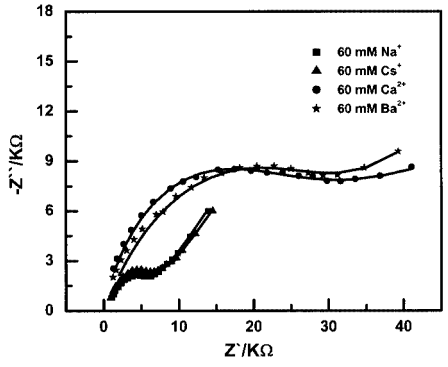

Figure 7. Comparative complex impedance plot for the SAMs of **3c** in the presence of Na^+, Cs^+, Ca^{2+} and Ba^{2+} (60 mM)

The fitting of all the impedance data was done with the program EQUIVALENT CIRCUIT.[29] Figure 8 shows a plot of ΔR_{ct} versus concentrations of different metal ions for SAMs of **3c**. SAMs of **3c** show a linear increase in R_{ct} with increased concentrations of $[Ca^{2+}]$ and $[Ba^{2+}]$. On the contrary, the same monolayer shows basically no response to Na^+, K^+ and Cs^+. In addition, the plot of ΔR_{ct} versus concentrations of $[Cs^+]$, $[Ca^{2+}]$ and $[Ba^{2+}]$ is shown in Figure 9. Both monolayers show a linear increase in R_{ct} with increased concentrations of $[Ca^{2+}]$ and $[Ba^{2+}]$ and exhibit a larger change in the presence of $[Ba^{2+}]$ than $[Ca^{2+}]$. Compared with SAMs of **3b**, SAMs of **3a** show better binding with Ca^{2+} and Ba^{2+}. Furthermore, SAMs of **3b** show a linear increase in R_{ct} with increased concentrations of $[Cs^+]$, but no response of $[Cs^+]$ for SAMs of **3a**. None of the SAMs **3a**−**3d** bind alkali metal ions, except **3b**, which has a suitable conformation and fit for Cs^+.

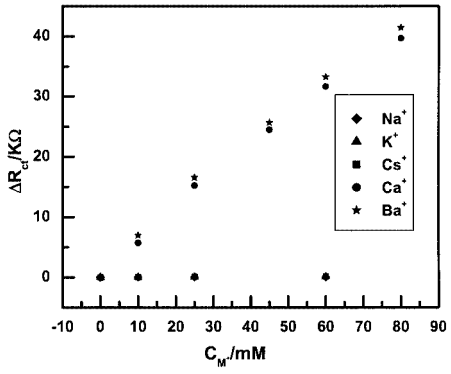

Figure 8. Plot of ΔR_{ct} versus concentrations of Na^+,K^+, Cs^+, Ca^{2+} and Ba^{2+} for SAMs of **3c**

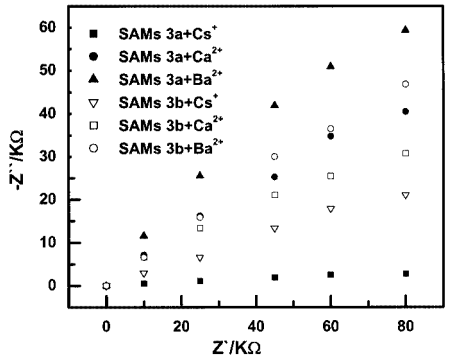

Figure 9. Comparative plot of ΔR_{ct} versus concentrations of Cs^+, Ca^{2+} and Ba^{2+} for SAMs of **3a** and **3b**

However, all of the SAM modified electrodes, including those from **3d**, efficiently bind Ca^{2+} and Ba^{2+}. Thus, complexation with the crown ether and the OEG chains are both possible. Attempts to determine the surface coverages of the different SAMs were not successful. However, experiments were designed to be self-consistent, since the same gold bead electrode was used to test the different metal cations. Also, different SAMs of the same calix[4]arene derivative exhibit the same recognition ability for metal cations. In this way, all the SAMs reported here are able to discriminate alkaline earth metal cations over alkali metal cations.

An effective synthetic procedure has been developed to prepare OEG chain attached *p-tert*-butylcalix[4]crown-6 derivatives and *p-tert*-butylcalix[4]arene disulfides. The self-as-

sembled monolayers of these disulfides were prepared and characterized by reflection-absorption infrared spectroscopy and contact angle measurements. Both RAIRS and contact-angle measurements prove that stable SAMs of these calix[4]arene derivatives can be formed on the gold surfaces. The metal cation recognition properties of these SAMs were investigated by electrochemistry and impedance spectroscopy. Although SAMs of **3b**, in the 1,3-alternate conformation, can bind with Cs^+ to some extent, all other SAMs show no recognition ability for alkali metal cations. However, all SAMs **3a**−**3d** serve as good sensors for alkaline earth metal cations such as Ca^{2+} and Ba^{2+}, as confirmed by CV blocking experiments and impedance spectroscopy. This work reports a group of sensors that are able to differentiate alkaline earth metal cations from alkali metal cations.

Experimental Section

Materials: Gold wire (99.999%) was obtained commercially. The gold substrates for RAIRS were prepared by vacuum deposition of gold (at a pressure of 10^{-7} Torr) on silica microslides. KCl, NaCl, CsCl, $CaCl_2$, KI, K_2CO_3, Ag_2O, TsCl, NaH, Cs_2CO_3, hexaammineruthenium(III) chloride, tetraethylammonium chloride, *p-tert*-butylcalix[4]arene and triethylene glycol were purchased and used as received. *p-tert*-Butylcalix[4]crown-6 and triethylene glycol monotosylate were synthesized as described in the literature.[22,24]

Electrochemical Measurements: Impedance and cyclic voltammetric measurements were performed by using a three-electrode cell with a gold bead as the working electrode, a coiled platinum mesh as the counter electrode and an aqueous Ag/AgCl solution as the reference electrode. Both electrochemical experiments were carried out with a CHI-660 electrochemical workstation. Impedance measurements were performed in a solution containing equal concentrations of oxidized and reduced forms of the $Ru(NH_3)_6^{3+/2+}$ redox couple. The formal redox potential [$E_{1/2} = (E_p^c + E_p^a)/2$] was determined by cyclic voltammetry. The frequency range utilized was 1 KHz to 0.1 Hz with an ac-amplitude of 5 mV. Impedance analysis was carried out by using the commercially available program EQUIVALENT CIRCUIT written by B. A. Boukamp (University of Twente). All experiments were carried out at room temperature with tetraethylammonium chloride (0.1 M) as the supporting electrolyte.

Infrared Spectroscopy: The transmission infrared spectra of the compounds were recorded from thin films prepared by putting a drop of the solution of the compound on a quartz cell and then evaporating under a flow of Ar; the spectra were obtained by using the same spectrometer with 500 scans and 4 cm^{-1} resolution. The reflection-adsorption infrared spectra were recorded on a Perkin−Elmer 2000 FT-IR spectrophotometer. The spectra were recorded with a liquid-nitrogen-cooled MCT detector, and the measurement chamber was continuously purged with argon gas during the measurements. Typically, 1000 scans with 4 cm^{-1} resolution were performed to get the average spectra. A clean and freshly prepared gold plate was used to record the reference spectrum.

Contact-Angle Measurements: Contact angles were measured with the contact-angle module of Multiskop (Optrel GBR, Guerickestr) at 293 K and ambient relative humidity. The contacting liquid (water) was dispensed and withdrawn using a 500 μL syringe at the slowest possible speed. For each type of monolayer, contact angles were collected and averaged from measurements on three separate slides using at least three drops per slide.

Monolayer Preparation: Gold-bead electrodes were prepared by heating the gold wire (99.999%) in a natural gas/O_2 flame until a small gold sphere formed on the end of the wire followed by cooling in deionized water (Barnstead 18 MΩ). This process results in the formation of well-defined Au (111) facets, as reported previously.[30] The gold wire was then sealed into a glass capillary leaving only the gold bead exposed. The gold beads were electrochemically cleaned by electrolysis in 0.1 M $HClO_4$ and the red crust that formed on the surfaces was removed by dipping them into 0.1 M HCl. The gold electrodes were then washed with copious amounts of water and acetonitrile. The geometric areas of the gold electrodes were calculated from the slopes of the linear plots of the cathodic peak current versus the square root of the scan rate obtained for the diffusion-controlled reduction of $Ru(NH_3)_6^{3+}$. Typical values for the geometric area of the electrode varied between 0.01−0.02 cm^2.

In a typical experiment, a monolayer was grown by dipping a freshly prepared gold bead into a deaerated acetonitrile solution of the appropriate thioctic ester derivative in 3 mM concentrations for 48 h to achieve optimum coverage. The substrates were then removed, rinsed with solvent and dried in a stream of Ar. SAM formation depends on the quality of the gold beads. About 80% of the gold beads with SAMs behave well and those are very stable under the measuring conditions.

Synthesis of 2c: *p-tert*-Butylcalix[4]crown-6 (0.25 g, 0.29 mmol) was dissolved in anhydrous DMF. NaH (28 mg, 1.16 mmol) was added to this solution and the mixture was stirred for 2 h at room temperature. Triethylene glycol monotosylate (0.4 g, 1.3 mmol) in DMF (5 mL) was then added very slowly over a period of 6 h at 60 °C. The reaction mixture was heated to 160 °C and stirred for 3 days. The solvent was removed and the residue was treated with 0.2 N acqueous HCl and CH_2Cl_2. The organic layer was dried over $MgSO_4$, filtered, evaporated and purified by column chromatography (SiO_2, 6−15% MeOH/ethyl acetate) to give a white solid **2c** (108 mg, 33%). The second band, eluted with 1:4 MeOH/ethyl acetate, was proved to be cone isomer **2a** (39 mg, 12%). ^1H NMR ($CDCl_3$): δ = 0.84 (s, 18 H), 1.33 (s, 9 H), 1.34 (s, 9 H), 3.17−3.22 (d, J = 12.8 Hz, 2 H), 3.55−4.32 (m, 44 H), 4.36−4.40 (d, J = 12.8 Hz, 2 H), 4.55−4.59 (d, J = 12.8 Hz, 2 H), 6.54 (s, 4 H), 7.03 (s, 2 H), 7.13 (s, 2 H) ppm. ^{13}C NMR ($CDCl_3$): δ = 30.6, 30.9, 31.6, 31.7, 33.6, 33.7, 34.0, 61.3, 69.7, 70.2, 70.3, 70.8, 70.9, 71.3, 71.5, 72.3, 72.6, 75.3, 124.6, 124.9, 125.5, 131.9, 132.2, 135.5, 140.6, 145.3, 145.7, 150.6, 151.2, 153.5 ppm. IR (CH_2Cl_2): $\tilde{\nu}$ = 2941, 2887, 2860, 1469, 1259, 1121, 974, 842, 750, 572 cm^{-1}.

Synthesis of 2d: *p-tert*-Butylcalix[4]arene (0.2 g, 0.29 mmol), triethylene glycol monotosylate (0.26 g, 0.86 mmol), K_2CO_3 (0.26 g, 1.85 mmol) and acetonitrile (20 mL) were refluxed under Ar for 48 h. After removing the solvent, the brownish residue was treated with 10% aqueous HCl and dichloromethane. The organic layer was washed three times with water and dried over anhydrous $MgSO_4$. After filtration and evaporation, the crude residue was chromatographed on silica gel using 5% MeOH/ethyl acetate as eluent to give a white solid **2d** (219 mg, 78%). ^1H NMR ($CDCl_3$): δ = 0.95 (s, 18 H), 1.31 (s, 18 H), 3.09 (s, broad, 2 H), 3.29−3.33 (d, J = 13.1 Hz, 4 H), 3.60−4.02 (m, 20 H), 4.16−4.18 (m, 4 H), 4.35−4.39 (d, J = 13.1 Hz, 2 H), 6.77 (s, 2 H), 7.07 (s, 4 H), 7.20 (s, 2 H) ppm. ^{13}C NMR ($CDCl_3$): δ = 30.9, 31.4, 31.7, 33.8, 33.9, 61.7, 69.9, 70.6, 70.9, 72.7, 75.4, 124.9, 125.4, 127.8, 132.5, 141.4,

146.8, 149.8, 150.4 ppm. IR (CH_2Cl_2): $\tilde{\nu}$ = 3470, 2933, 2894, 2847, 1473, 1257, 1120, 766, 530 cm^{-1}.

General Synthetic Procedure for 3a−3d: The alcohol-functionalized *p-tert*-butylcalix[4]crown-6 and *p-tert*-butylcalix[4]arene derivatives **2a−2d** and thioctic acid (3 molar equiv.) were dissolved in CH_2Cl_2 (5 mL). The mixture was stirred for 30 min at 0 °C under Ar. Then, 1,3-dicyclohexylcarbodiimide (DCC; 4 molar equiv.) and 4-(dimethylamino)pyridine (DMAP; 0.6 molar equiv.) were added, and the mixture was stirred for another 30 min at 0 °C. The cooling bath was then removed and the solution allowed to warm to room temperature. After stirring for 48 h under Ar, the reaction mixture was filtered through a fine glass frit to afford a clear filtrate and the insoluble urea by-product as a white solid. The filtrate was washed three times with water and dried over $MgSO_4$. After filtration and evaporation, the residue was subjected to column chromatography.

3c: Prepared from **2c** (0.10 g, 0.09 mmol) and purified by column chromatography (SiO_2, 1:1 CH_2Cl_2/ethyl acetate) to give a pale-yellow solid **3c** (102 mg, 76%). M.p. 82.3−83.7 °C. ^{1}H NMR ($CDCl_3$): δ = 0.83 (s, 18 H), 1.31 (s, 9 H), 1.32 (s, 9 H), 1.46−1.49 (m, 4 H), 1.63−1.70 (m, 8 H), 1.82−1.97 (m, 2 H), 2.31−2.33 (m, 4 H), 2.34−2.38 (m, 2 H), 3.09−3.19 (m, 8 H), 3.53−4.34 (m, 44 H), 4.31−4.35 (d, J = 13 Hz, 2 H), 4.53−4.57 (d, J = 13 Hz, 2 H), 6.53 (s, 4 H), 7.00 (s, 2 H), 7.10 (s, 2 H) ppm. ^{13}C NMR ($CDCl_3$): δ = 30.7, 31.1, 31.7, 31.8, 33.7, 33.8, 33.9, 34.1, 34.6, 38.5, 40.2, 56.3, 63.6, 69.2, 69.9, 70.3, 70.4, 70.9, 71.1, 71.6, 72.4, 75.4, 124.7, 124.9, 125.1, 125.6, 128.6, 132.1, 132.3, 135.6, 140.8, 145.4, 145.7, 150.7, 151.4, 153.6, 173.5, 178.5 ppm. MS (MALDI): m/z = 1513.4 [M^+ + Na], 1529.3 [M^+ + K]. IR (CH_2Cl_2): $\tilde{\nu}$ = 2930, 2905, 2854, 1731, 1482, 1461, 1122, 843, 735, 560 cm^{-1}. $C_{82}H_{122}O_{16}S_4 \cdot H_2O$: calcd. C 65.22, H 8.28; found C 65.45, H 8.17.

3d: Prepared from **2d** (0.25 g, 0.22 mmol) and purified by column chromatography (SiO_2, 10% ethyl acetate/CH_2Cl_2) to give a pale-yellow viscous oil **3d** (0.23 g, 82%). ^{1}H NMR ($CDCl_3$): δ = 0.94 (s, 18 H), 1.30 (s, 18 H), 1.45−1.50 (m, 4 H), 1.63−1.70 (m, 8 H), 1.90−1.94 (m, 2 H), 2.32−2.37 (t, J = 7.4 Hz, 4 H), 2.37−2.43 (m, 2 H), 3.10−3.17 (m, 4 H), 3.27−3.31 (d, J = 12.8 Hz, 2 H), 3.57−3.67 (m, 2 H), 3.70−3.74 (m, 8 H), 3.82−3.85 (m, 4 H), 3.95−3.98 (m, 4 H), 4.15−4.20 (m, 8 H), 4.34−4.38 (d, J = 12.8 Hz, 2 H), 6.77 (s, 4 H), 7.05 (s, 4 H), 7.15 (s, 2 H) ppm. ^{13}C NMR ($CDCl_3$): δ = 31.0, 31.5, 31.8, 33.9, 34.6, 38.5, 40.2, 56.4, 63.6, 69.3, 70.1, 70.8, 71.0, 75.3, 125.1, 125.5, 127.9, 132.5, 141.4, 144.4, 149.7, 150.6, 173.9 ppm. MS (MALDI): m/z = 1327.1 [M^+ + K]. IR (CH_2Cl_2): $\tilde{\nu}$ = 3354, 2928, 2905, 2847, 1737, 1462, 1123, 845, 730, 558 cm^{-1}. $C_{72}H_{104}O_{12}S_4 \cdot H_2O$: calcd. C 67.05, H 8.13; found C 67.27, H 8.43.

Supporting Information: Synthetic procedures and spectroscopic data for **2a**, **2b**, **3a** and **3b** are available from the author upon request (see also the footnote on the first page of this article).

Acknowledgments

Financial support from the National Science Foundation (Grant No. CHE-0135786) is greatly appreciated.

[1] D. D. Offord, S. B. Sachs, M. S. Ennis, T. A. Eberspacher, J. H. Griffin, C. E. D. Chidsey, J. P. Collman, *J. Am. Chem. Soc.* **1998**, *120*, 4478−4487.
[2] D. Philp, F. Stoddart, *Angew. Chem. Int. Ed. Engl.* **1996**, *35*, 1155−1196.
[3] Y. G. H. Weizman, J. L. A. Shanzer, I. Rubinstein, *Chem. Eur. J.* **1996**, *2*, 759−766.
[4] I. Rubinstein, S. Steinberg, Y. Tor, A. Shanzer, J. Sagiv, *Nature* **1998**, *332*, 426−428.
[5] [5a] C. Henke, C. Steinem, A. Janshoff, G. Steffan, H. Lufthmann, M. Sieber, H.-J. Galla, *Anal. Chem.* **1996**, *68*, 3158−3165. [5b] E. Katz, I. Willner, *Electroanalysis* **2003**, *15*, 913−947.
[6] [6a] T. Adams, F. Davis, C. J. M. Stirling, *J. Chem. Soc., Chem. Commun.* **1994**, 2527−2530. [6b] F. Davis, C. J. M. Stirling, *Langmuir* **1996**, *12*, 5365−5374.
[7] A. Friggeri, F. C. J. M. Van Veggel, D. N. Reinhoudt, R. P. H. Kooyman, *Langmuir* **1998**, *14*, 5457−5463.
[8] M. T. Rojas, R. Koeniger, J. F. Stoddart, A. E. Kaifer, *J. Am. Chem. Soc.* **1995**, *117*, 336−343.
[9] A. J. Moore, L. Goldenberg, M. R. Bryce, M. C. Petty, A. P. Monkman, S. N. Port, *Adv. Mater.* **1998**, *10*, 395−398.
[10] S. Flink, B. A. Boukamp, A. Van den Berg, F. C. J. M. van Veggel, D. N. Reinhoudt, *J. Am. Chem. Soc.* **1998**, *120*, 4652−4657.
[11] K. Brandyopadhyay, H. Liu, S.-G. Liu, L. Echegoyen, *Chem. Commun.* **2000**, 141−142.
[12] H. Liu, S.-G. Liu, L. Echegoyen, *Chem. Commun.* **1999**, 1493−1494.
[13] B. Colonna, L. Echegoyen, *Chem. Commun.* **2001**, 1104−1105.
[14] P. R. A. Webber, A. Cowley, M. G. B. Drew, P. D. Beer, *Chem. Eur. J.* **2003**, *9*, 2439−2446.
[15] K. Iwamoto, S. Shinkai, *J. Org. Chem.* **1992**, *57*, 7066−7073.
[16] A. Casnati, A. Pochini, R. Ungaro, C. Bocchi, F. Ugozzoli, R. J. M. Egberink, H. Struijk, R. Lugtenberg, F. de Jong, D. N. Reinhoudt, *Chem. Eur. J.* **1996**, *2*, 436−445.
[17] R. A. Sachleben, A. Urvoas, J. C. Bryan, T. J. Haverlock, B. P. Hay, B. A. Moyer, *Chem. Commun.* **1999**, 1751−1752.
[18] R. Ungaro, A. Casnati, F. Ugozzoli, A. Pochini, J.-f. Dozol, C. Hill, N. Rouquette, *Angew. Chem. Int. Ed. Engl.* **1994**, *33*, 1506−1509.
[19] Z. Asfari, J. Weiss, S. Pappalardo, J. Vicens, *Pure Appl. Chem.* **1993**, *65*, 585−590.
[20] H.-F. Ji, E. Finot, R. Dabestani, T. Thundat, G. M. Brown, P. F. Britt, *Chem. Commun.* **2000**, 457.
[21] S. Zhang, L. Echegoyen, *Tetrahedron Lett.* **2003**, *44*, 9079−9082.
[22] E. Ghidini, F. Ugozzoli, R. Ungro, S. Harkema, A. A. El-Fadl, D. N. Reinhoudt, *J. Am. Chem. Soc.* **1990**, *112*, 6979−6985.
[23] J. S. Kim, W. K. Lee, S. H. Lee, J.-G. Kim, I.-H. Suh, J. Y. Kim, J. W Kim, *J. Incl. Phenom.* **2001**, *40*, 183−187.
[24] A. Bouzide, G. Sauve, *Org. Lett.* **2002**, *4*, 2329−2332.
[25] A. Casnati, A. Pochini, R. Ungaro, F. Ugozzoli, F. Arnaud, S. Fanni, J.-J. Schwing, R. J. M. Egberink, F. de Jong, D. N. Reindoudt, *J. Am. Chem. Soc.* **1995**, *117*, 2767−2777.
[26] J. S. Kim, J. H. Pang, I. H. Suh, D. W. Kim, D.W. Kim, *Synth. Commun.* **1998**, *28*, 677−683.
[27] J. D. Faull, V. K. Gupta, *Langmuir* **2001**, *17*, 1470−1476.
[28] H. O. Finklea, D. A. Snider, J. Fedyk, E. Sabatani, Y. Gafni, I. Rubinstein, *Langmuir* **1993**, *9*, 3660−3667.
[29] S. Flink, F. C. J. M. van Veggel, D. N. Reinhoudt, *J. Phys. Chem. B* **1999**, *103*, 6515−6520.
[30] J. Schneir, R. Sonnenfeld, Q. Marti, P. K. Hansma, J. E. Demuth, R. J. hamers, *J. Appl. Phys.* **1988**, *63*, 717−721.

Received February 24, 2004

